Absorbed current electron spin polarization detector

D. T. Pierce, S. M. Girvin, J. Unguris,[a] and R. J. Celotta

National Bureau of Standards, Washington, D.C. 20234

(Received 18 May 1981; accepted for publication 24 June 1981)

The principle of spin analysis by means of measurement of the spin dependent absorption of a polarized electron beam is presented. The spin dependent signal is enhanced relative to the spin averaged signal at an energy near which the secondary yield is unity. Both the collected charge method and the zero-crossing method are described for situations where the polarization can and cannot be reversed. A statistical analysis of the uncertainty in the polarization determination by each method is given. Annealed, evaporated Au films are shown to be suitable for the detecting surface of this spin detector. The figure of merit is derived and found for Au films to be comparable to the very best Mott detectors, but the electron optical acceptance is smaller. The applications for which this simple compact spin detector are especially suited are discussed.

PACS numbers: 07.55. + x, 79.20.Hx

INTRODUCTION

A new type of electron spin polarization detector based on the spin dependent absorption of a polarized electron beam incident on a surface has recently been discussed.[1-3] A unique feature of this detector is the large enhancement of the spin-dependent signal relative to the spin averaged signal near the energy, where the secondary electron yield is unity. While the minimization of the spin averaged background signal can be experimentally advantageous, with appropriate calibration this type of detector could operate over a wide range of energy. This spin-dependent absorption was discovered[1] in an investigation of spin polarized electron scattering from a ferromagnetic glass, $Ni_{40}Fe_{40}B_{20}$, where the spin dependence is due to the exchange interaction between the incident electron spin and the aligned spins in the surface. It was noted[1] that a large spin-dependent absorption should also occur due to the spin-orbit interaction as has since been observed for Au(110)[2] and W(100)[3] single crystal surfaces.

A comprehensive discussion of the principle of this spin detector and its two primary modes of operation, charge collection and zero crossing measurement, is given in the next section. Although high efficiency has been claimed for this spin detector,[2,3] a statistical analysis of the detector efficiency has been lacking. In Sec. II, we present a detailed statistical analysis of the uncertainty in polarization measurement for both detector modes. For a practical spin detector, it is desirable to avoid problems associated with preparation and alignment of single crystal surfaces. We have investigated the spin-dependent absorption in evaporated Au films which are easily prepared, stable, and efficient for spin detection. These results are presented in Sec. III. Both the statistical analysis of the detector efficiency and the experimental results from Au films influence the design and application of such a detector as discussed in Sec. IV.

I. PRINCIPLES OF OPERATION

The spin dependence of elastic scattering of a spin polarized electron beam from a surface as a result of the spin-orbit interaction and, in the case of magnetic surfaces, as a result of the exchange interaction, has been investigated for a number of materials.[4] The current collected by the sample, i.e., absorbed, has been found to be spin dependent primarily due to the spin dependence of the elastic scattering. When electrons of one spin orientation are preferentially scattered, the opposite spin orientation is preferentially absorbed.[1]

Usually, one measures the net absorbed electron current I_a (electron/s) for an unpolarized incident beam. The net absorbed current consists of the primary electrons incident on the sample minus the elastically and inelastically backscattered primaries and the low energy true secondaries. At an energy E_o, where the secondary yield is unity, the absorbed current is zero; the number of electrons leaving the sample is equal to the number reaching it. Note that secondary yield as customarily defined includes all electrons leaving the sample including those elastically scattered. At energies just above E_o, more electrons leave the crystal and the net electron current absorbed is negative. (Our discussion concerns the lower energy where the secondary yield is unity; this also occurs at another higher energy, but the spin dependence is small there.) A measurement of I_a is shown in Fig. 1 for a beam incident on an annealed, evaporated Au film (Sec. III) at an angle of incidence $\alpha = 25°$.

For a 100% polarized incident electron beam, a net absorbed current $i^{\uparrow}$ ($i^{\downarrow}$) is measured for the incident electron spin polarization parallel (antiparallel) to the quantization direction. The quantization direction for a ferromagnetic surface is taken to be the majority spin direction (i.e., opposite to the magnetization). When the spin dependence is due to the spin orbit interaction, the

 0034-6748/81/101437-08$00.60

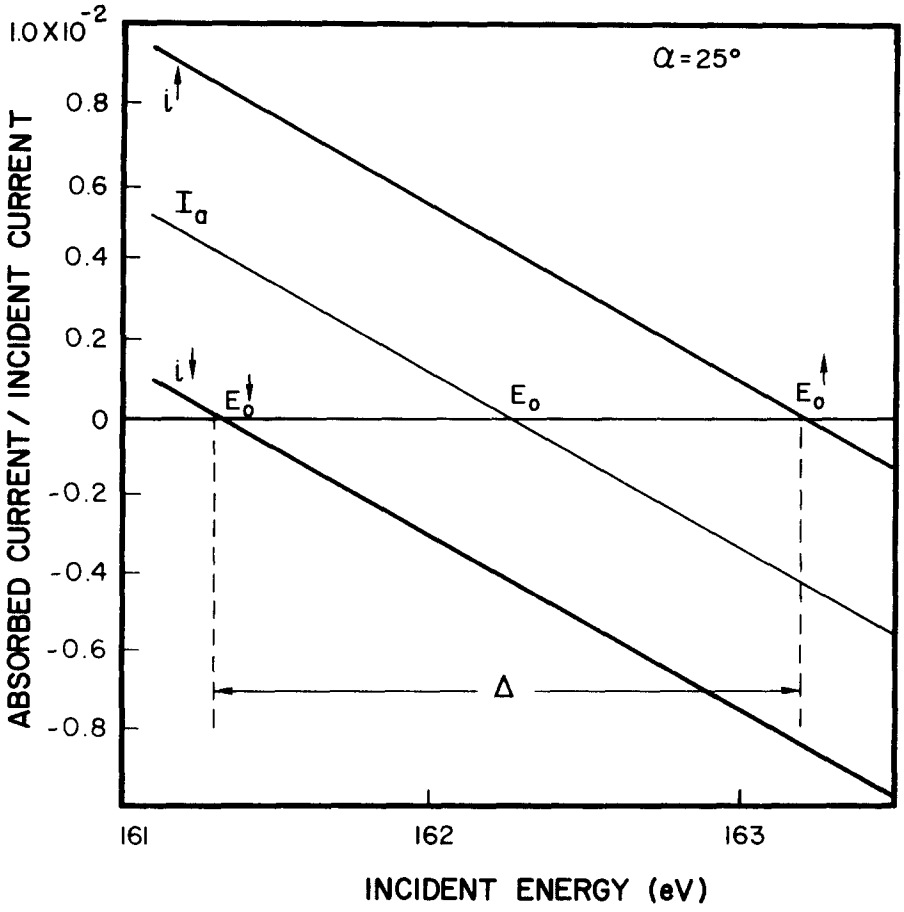

FIG. 1. The electron current $i^{\uparrow}$ and $i^{\downarrow}$ as a function of incident energy absorbed by an annealed evaporated Au film when it intercepts, at an angle of incidence of 25°, a completely polarized electron beam with polarization parallel and antiparallel to the normal to the scattering plane respectively. The current absorbed by an unpolarized or spin-averaged beam is given by $I_a = (i^{\uparrow} + i^{\downarrow})/2$. The secondary yield equals unity at a different energy for each polarization of the incident beam. The difference in energy between $i^{\uparrow} = 0$ and $i^{\downarrow} = 0$ is defined Δ.

quantization direction is taken to be the normal to the scattering plane $\hat{n} = (\mathbf{k} \times \mathbf{k}')/|\mathbf{k} \times \mathbf{k}'|$, where $\mathbf{k}$ and $\mathbf{k}'$ are the initial and final wavevectors of a specularly reflected electron. In the case of the spin-orbit interaction, there is no spin dependence at normal incidence, i.e., $i^{\uparrow} = i^{\downarrow}$. Figure 1 shows $i^{\uparrow}$ and $i^{\downarrow}$ corresponding to a 100% polarized beam incident on the Au film.

The essential feature of the spin-dependent absorbed current in Fig. 1 is that the secondary yield is unity at two different energies, $E_o^{\uparrow}$ and $E_o^{\downarrow}$, for incident beam polarization, respectively, parallel and antiparallel to the quantization direction. This energy difference, $|E_o^{\uparrow} - E_o^{\downarrow}|$, we define as Δ. At an energy $E_o^{\downarrow}$ where $i^{\downarrow} = 0$, on the average only incident spins parallel to the quantization direction give rise to a net absorbed current; in this sense the absorption acts as a perfect spin filter. This result is analogous to having a Sherman function of unity in Mott scattering.[5] We define a parameter $\eta \equiv |i^{\uparrow} - i^{\downarrow}|/I_o$, where I_o is the incident current. For a 100% polarized incident beam at $E_o^{\downarrow}$ or $E_o^{\uparrow}$, η, is just the ratio of the absorbed current to the incident current and may be of order 1%.

In previous work[1] on $Ni_{40}Fe_{40}B_{20}$, we investigated the origin of the difference in the energies at which the secondary yield is unity for the two directions of polarization of the incident beam. The production of true secondaries was found to be independent of the polarization of the incident beam. The spin dependence of the secondary yield (in the general sense of all electrons leaving the sample), and therefore of the absorbed current, was associated with the spin dependence in the elastic scattering of the primary beam.

The curves $i^{\uparrow}$ and $i^{\downarrow}$ of Fig. 1 are measurements at 0.1 eV intervals connected by lines. The scatter of the points is less than the line width. The curves are measured with a beam of known polarization and corrected to correspond to a beam of 100% polarization.[4] In the case illustrated, the curves are nearly parallel and $E_o \simeq \frac{1}{2}|E_o^{\uparrow} - E_o^{\downarrow}|$. Such behavior is not necessary for a surface to be useful as a detector as long as the behavior is known from an accurate calibration measurement.

For discussion of the modes of detector operation and a statistical analysis of its efficiency, we refer to Fig. 2. In Fig. 2, we consider the number of electrons collected, i.e., absorbed, in a given time. The energy dependence of the charge collected is shown for four different polarizations of the incident beam, +1, $+P$, $-P$, and −1 where P is an arbitrary unknown polarization. To simplify our discussion, Fig. 2 is an idealized version of Fig. 1 in that the four curves are assumed parallel and linear with E_o centered between the zero crossings. The collected charge curves $Q_+(E)$ and $Q_-(E)$ corresponding to a polarization of $+P$ and $-P$ cross zero at $E_o(+P)$ and $E_o(-P)$, respectively. If there are M primary electrons incident on the detector surface, the separation between the curves for

incident polarization +1 and −1 corresponds to a charge ηM.

The detector is characterized by the parameters η, Δ, and E_o. The parameters η and Δ are determined by a calibration measurement using an electron beam of known polarization. The energy, E_o, the value of which is influenced primarily by the low energy secondary electrons, may vary during the course of an experiment due to small changes in the work function of the detector surface or changes in electric fields at the surface caused by neighboring electrodes. On the other hand, the quantities, η and Δ, which are determined primarily by the elastically scattered electrons, are insensitive to these changes.

There are several modes of operation of such a detector which can be classified as to whether the polarization is reversible or not and as to whether the net collected charge, or the energy at which the collected charge is zero, is measured. When the polarization is reversible, such that it is possible to measure both $Q_+(E)$ and $Q_-(E)$, then knowing η and Δ, it is possible to determine P without knowing E_o accurately. This can be advantageous in situations where it is not straightforward to obtain an unpolarized beam needed to measure E_o should it vary during an experiment.

A. Polarization reversible

In many cases experimental parameters, e.g., the polarization of the incident beam or the magnetization of the sample, can be modified to reverse the polarization to be analyzed. Alternatively, the quantization direction of the detector may be reversed. When the detector is a ferromagnetic surface, this is accomplished by reversing the magnetization. In the case of the spin-orbit interaction, the same effect is achieved by changing the angle of incidence from $+\alpha$ to $-\alpha$, thereby reversing the normal to the scattering plane.

1. Collected charge method

The absorbed charge, $Q_+(E)$ and $Q_-(E)$, is measured for the two polarizations at an energy E in the neighborhood of E_o. The total incident charge M can be measured to a good approximation by applying a positive bias to the detector surface. The polarization is obtained from

$$P = (Q_+ - Q_-)/\eta M. \tag{1}$$

Strictly speaking, this measurement is independent of E_o only if the curves of Fig. 2 are parallel. Otherwise it would be necessary to know the difference between the measurement energy and E_o in order to make use of calibration curves.

Another method may be useful in some applications. This utilizes the polarization reversal to eliminate the need to measure total incident charge, but the measurement must be made at a particular energy, e.g., $E_o - \Delta/2$, and therefore E_o must be known. At this energy the polarization is given by

$$P = (Q_+ - Q_-)/(Q_+ + Q_-). \tag{2}$$

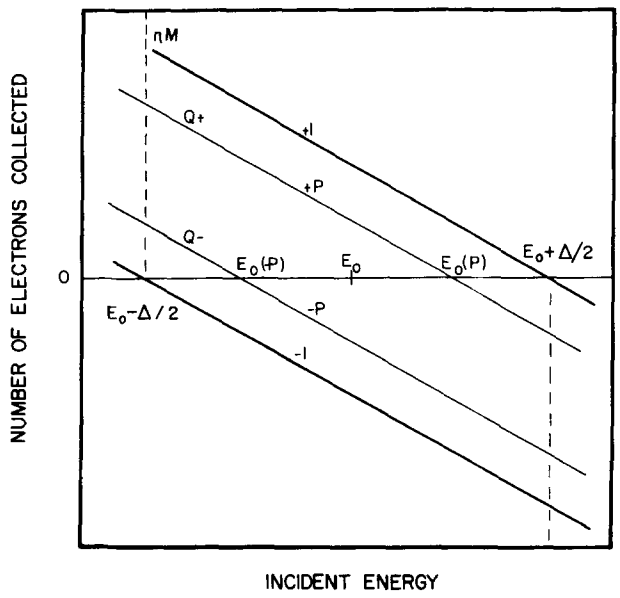

FIG. 2. An idealized schematic of Fig. 1 where now the current absorbed over a period of time (number of electrons collected) is plotted vs energy for four different incident beam polarizations: +1, P, $-P$, −1. The number of incident electrons is M. In the charge collection method of spin polarization determination, Q_+ and Q_- are measured. In the zero-crossing method, $E_o(\pm P)$ is measured.

2. Zero crossing method

This method involves measuring the energies $E_o(P)$ and $E_o(-P)$ at which the net absorbed charge is zero for positive and negative polarization, respectively. The difference between these energies is then simply related to the unknown polarization by

$$P = [E_o(P) - E_o(-P)]/\Delta. \tag{3}$$

B. Polarization not reversible

In this type of experiment the absorbed current is measured as a function of energy for only one sign of the polarization. Methods, similar to the ones discussed above, can be applied to the measurement of the polarization, if in addition to η or Δ, E_o is also known.

1. Collected charge method

The polarization can be determined by measuring the net absorbed charge and the number of incident electrons at exactly E_o. The polarization is given by

$$P = [2Q_+(E_o)]/\eta M. \tag{4}$$

A second method makes use of Eq. (2), even though the polarization cannot be reversed. From Fig. 2 it can be seen that Q_+ and Q_- required for Eq. (2) can be determined by measuring the charge at both $E_o - \Delta/2$ and $E_o + \Delta/2$.

2. Zero crossing method

If the energy at which the net absorbed current is zero is measured and E_o is known, the polarization can be determined from

$$P = [E(P) - E_o]/\Delta/2. \tag{5}$$

II. STATISTICAL ANALYSIS OF DETECTOR EFFICIENCY

The uncertainty in a measurement of P with an absorbed current spin polarization detector has contributions from fluctuations in the current of the incident electron beam and from fluctuations associated with secondary electron production. Fluctuations in secondary production are of interest in connection with noise in electron tubes and electron multipliers, and the subject has been discussed in a number of early papers.[6-9] The net absorbed current is the difference between two large currents, the incident and the secondary electron currents. Therefore, the root mean square deviation in a measurement of Q_+, for example, is larger than the value $\sqrt{Q_+}$ expected for random noise in the collected charge.

A. Fluctuation in Q

We first derive an expression for the fluctuation in Q and then derive the statistical noise associated with a measurement of the polarization by each of the methods described above.

Each of the M primary electrons incident on the detector can produce 0, 1, 2, 3 . . . etc., up to a very large number of secondary electrons. Let the ith primary produce n_i secondaries and let the mean and mean square values of n_i be $\bar{n}$ and $\overline{n^2}$, respectively. The net number of electrons collected is

$$Q = \sum_{i=1}^{M} (1 - n_i). \tag{6}$$

Averaging this over the distribution of secondaries yields

$$\bar{Q} = M(1 - \bar{n}). \tag{7}$$

The number of primaries M can fluctuate from run to run. Denoting the average of M over an ensemble of runs by brackets, one obtains

$$\langle \bar{Q} \rangle = \langle M \rangle (1 - \bar{n}), \tag{8}$$

and

$$\langle \bar{Q} \rangle^2 = \langle M \rangle^2 (1 - \bar{n})^2. \tag{9}$$

Likewise the square of the number of collected electrons is

$$Q^2 = \sum_{i=1}^{M} (1 - n_i)^2 + \sum_{i \neq j} \sum_{j=1}^{M} (1 - n_i)(1 - n_j). \tag{10}$$

Averaging over the secondaries leaves

$$\overline{Q^2} = M(1 - 2\bar{n} + \overline{n^2}) + M(M - 1)(1 - \bar{n})^2, \tag{11}$$

assuming n_i and n_j are statistically independent for $i \neq j$.

Averaging the primaries over an ensemble of runs yields

$$\langle \overline{Q^2} \rangle = \langle M^2 \rangle (1 - \bar{n})^2 + \langle M \rangle (\overline{n^2} - \bar{n}^2). \tag{12}$$

The fluctuations $\langle \overline{\delta Q^2} \rangle$ in Q are

$$\langle \overline{Q^2} \rangle - \langle \bar{Q} \rangle^2 = [\langle M^2 \rangle - \langle M \rangle^2] (1 - \bar{n})^2 + \langle M \rangle (\overline{n^2} - \bar{n}^2). \tag{13}$$

The first term is due to noise in the primary beam while the second is due to fluctuations in secondary production. Note that if it were possible for each primary to generate exactly $\bar{n}$ secondaries, then the second term would be zero. Assuming the number of primaries is Gaussian distributed,

$$\langle \overline{\delta Q^2} \rangle = \langle M \rangle [(1 - \bar{n})^2 + (\overline{n^2} - \bar{n}^2)]. \tag{14}$$

This is in agreement with the results of Campbell.[10]

B. Fluctuations in P: charge collection method

We are now in a position to estimate the error in the measured polarization due to fluctuations in Q. We consider first the charge collection method and use Eq. (1). Referring to Fig. 2 and using Eq. (1), the average charge collected at an energy E_0 is

$$\bar{Q}_\pm = \bar{M}(1 - \bar{n}_\pm) = \pm P \bar{M} \eta / 2, \tag{15}$$

where we no longer distinguish between the bar and bracket averages. Here $\bar{n}_+$ corresponds to the average number of electrons leaving the detector for each incident electron of a beam with polarization P. We make the calculation at E_o only for convenience. Using (14) and (15), the mean square fluctuation in collected charge is given by

$$\overline{\delta Q_\pm^2} = \bar{M} \left(\frac{\eta^2 P^2}{4} + \delta^2 \right), \tag{16}$$

where

$$\delta^2 \equiv \overline{n^2} - \bar{n}^2 \tag{17}$$

is assumed to be polarization independent. The corresponding error in the polarization is given by

$$\overline{\delta P^2} = \left(\frac{\partial P}{\partial Q_+} \right)^2 \overline{\delta Q_+^2} + \left(\frac{\partial P}{\partial Q_-} \right)^2 \overline{\delta Q_-^2} + \left(\frac{\partial P}{\partial M} \right)^2 \overline{\delta M^2} + \left(\frac{\partial P}{\partial \eta} \right)^2 \overline{\delta \eta^2}. \tag{18}$$

We assume that η is determined as precisely as required from a calibration measurement so the last term is negligible. Then the error in P can be written

$$\overline{\delta P^2} = \frac{3P^2}{2\bar{M}} + \frac{2\delta^2}{\bar{M}\eta^2}. \tag{19}$$

Since $\eta^2/\delta^2 \ll 1$ the latter term which derives from fluctuations in the secondary current dominates and

$$\overline{\delta P^2} = \frac{2\delta^2}{\bar{M}\eta^2}. \tag{20}$$

Equation (20) remains applicable for operation at an energy E away from E_o over a range depending on the calibration curve. For a linear curve, as in Fig. 2, Eq. (20) is valid as long as $\eta|E - E_o|/\Delta \ll 1$. We note that for P determined from Eq. (2) one finds a result similar to Eq. (20), i.e., $\overline{\delta P^2} = 2\delta^2(1 + P^2)/\eta^2\bar{M}$.

C. Fluctuations in P: zero-crossing method

The second method of polarization determination consists of measuring the primary energy $E_o(\pm P)$ at which $Q_\pm$ vanishes and then using Eq. (3). For each polarization direction the intercept is determined by measuring Q_i at a sequence of N energies, E_i, and fitting the data to a straight line. Assuming $\eta^2/\delta^2 \ll 1$ so that

$$\overline{\delta Q_i^2} = \delta^2\bar{M} \tag{21}$$

standard linear regression analysis[11] yields

$$\overline{\delta E_0(\pm P)^2} = \frac{\delta^2\bar{M}}{\beta^2}\left(\frac{1}{N} + \frac{R^2}{T\beta^2}\right), \tag{22}$$

where

$$R \equiv \frac{1}{N}\sum_i Q_i, \tag{23}$$

$$T \equiv \sum_i (E_i - T_0)^2, \tag{24}$$

and

$$T_0 \equiv \frac{1}{N}\sum_i E_i. \tag{25}$$

The slope of the line is

$$\beta = \eta\bar{M}/\Delta. \tag{26}$$

The second term in (22) can be made negligibly small ($\lesssim 1/N$) by suitable choice of the energies E_i; i.e., by bracketing closely the zero crossover. Hence using (3) we have

$$\overline{\delta P^2} = \frac{2}{\Delta^2}\overline{\delta E_0(\pm P)^2} \simeq \frac{2\delta^2}{\eta^2\bar{M}N}. \tag{27}$$

D. Typical detector parameters

The mean square deviations in the polarization measurements by the two methods are seen to be quite similar. There is a factor $1/N$ in Eq. (27), but the measurement then takes N times longer since the number of incident electrons is $2N\bar{M}$ instead of $2\bar{M}$ for the charge collection method. It should be noted that we have assumed in both cases that the detector has been previously calibrated to determine Δ and η with negligible statistical error. It is straightforward to work out the error in P in the case where the polarization is not reversible and is determined from Eqs. (4) and (5). For the charge collection method of Eq. (4) we find $\overline{\delta P^2} \simeq 4\delta^2/\eta^2\bar{M}$ which is twice as large as $\overline{\delta P^2}$ in Eq. (20), but the measurement takes only half as long since only Q_+ *or* Q_- is measured, not both. For the zero crossing method of Eq. (5), one obtains the same result for $\overline{\delta P^2}$ as in Eq. (27), if the error in measuring E_o is included.

To evaluate the fluctuations in P from Eqs. (20) and (27) we need to know the value of $\delta^2 = \overline{n^2} - \bar{n}^2$. Measurements of δ^2 for several materials have been made by comparing the secondary emission fluctuations in the plate current of a triode vacuum tube to the temperature limited shot noise of a reference diode tube.[6-8] For efficient secondary emitters such as BaO or SrO at energies several times E_o, values of δ^2 up to about 20 were measured. For a metal surface such as Ni at energies near E_o, the measurements[7] give $\delta^2 \simeq 1$. Such a value is appropriate for the spin detector we are considering. It may be noted that if the secondary emission is assumed to follow Poisson's formula, then $\delta^2 = \bar{n} \approx 1$ since $1 - \bar{n} \ll 1$; from the results cited, it is clear that secondary emission may depart from Poisson's formula.[9]

The root mean square deviation in measurement of polarization is from Eq. (20)

$$(\overline{\delta P^2})^{1/2} \approx (\eta^2\bar{M})^{-1/2}, \tag{28}$$

where for the purpose of discussion we approximate the factor $2\delta^2$ by unity. Typical values of η are of order 10^{-2}. The value of η in Fig. 1 is 0.0086. This is near the maximum value we have observed for such an Au film as discussed in Sec. III. Values of η reported[2,3] for $Ni_{40}Fe_{40}B_{20}$, Au(110), and W(100), respectively, were 0.006, 0.010, and 0.008 at respective angles of incidence of 0°, 56.5°, and 14°. Thus from Eq. (28) with $\eta = 10^{-2}$, in order to achieve an rms deviation of 1%, 10^8 incident electrons are required.

In comparing spin detectors, figures of merit are often quoted. For a scattering type detector such as a Mott detector[5] or a polarized low energy electron diffraction (PLEED) spin detector,[12,13] the rms deviation in a polarization measurement is

$$(\overline{\delta P^2})^{1/2} = (IS^2)^{-1/2}, \tag{29}$$

where I is the scattered electron intensity and S is the Sherman function, a measure of the spin dependent scattering asymmetry. The figure of merit, S^2I/I_o, where I_o is the incident beam intensity is seen from Eq. (29) to equal $(\overline{\delta P^2}I_o)^{-1}$. For the absorption detector with the approximations of Eq. (28), we have for the figure of merit

$$(\overline{\delta P^2}I_o)^{-1} \approx \eta^2. \tag{30}$$

The figure of merit for the absorption spin detector with $\eta = 10^{-2}$ is 10^{-4}; this is about the same as the figure of merit of a PLEED detector or an optimized Mott detector and an order of magnitude greater than a typical Mott detector. The advantages of the absorbed current spin detector are its simplicity and convenience for certain measurements as discussed in Sec. IV.

III. EXPERIMENTAL RESULTS FOR EVAPORATED Au FILMS

As a material for an absorbed current spin detector, gold has several desirable attributes. It is a high-Z material where the spin-orbit interaction is expected to

be large; this has been observed in the measurements of Erbudak and Muller[2] for Au(110) and in our measurements of Au(110) and Au(111) crystal surfaces. The Au surface is also relatively inert so that changes due to contamination in the vacuum system should be small. However, Au crystals are soft and difficult to polish. To clean the surface in the vacuum chamber, ion bombardment and annealing is required; this could be an inconvenient constraint in the design of a compact, moveable detector. On the other hand, clean Au films are very easy to prepare by evaporation. We made measurements on (1) an air-exposed Au film as installed, (2) freshly evaporated Au films, and (3) films which were annealed after evaporation. Seven evaporated films were measured in all.

Data like that illustrated in Fig. 1 for $\alpha = 25°$ were obtained for many angles of incidence. Such measurements of $i^{\uparrow}$, $i^{\downarrow}$, and $I_a = (i^{\uparrow} + i^{\downarrow})/2$ in an energy range around E_o determine the three important parameters for the spin detector: E_o, Δ, and η. Measurements were made with a spin polarized electron gun and surface analysis chamber previously described.[13,14] For these measurements a special manipulator was used which allowed variation of the angle of incidence $\pm 75°$ from normal. In this configuration it was not possible to make use of the Auger spectroscopy capability. The initial substrate was a polished Mo surface which capped a cylinder enclosing the heating filament. The Au films were evaporated from a Joule-heated Mo boat onto the existing films. The base pressure of the system was 5×10^{-11} Torr and rose to the 10^{-8} Torr range during evaporation.

An air-exposed Au film was measured after a normal bakeout (~24 h at 180 °C). The values for E_o at all angles were about 50 eV lower than for the clean annealed films discussed below. The values of Δ and η were closer to the annealed films discussed below than the freshly evaporated ones. For example, for the air-exposed film at $\alpha = 25°$, we found $\eta = 0.006$ and $\Delta = 1.8$ eV. However, even a low intensity 0.1 μA electron beam at 150 eV caused E_o to increase about 1 eV per minute; E_o did not change with the beam off. The change in E_o only took place at the position of the electron beam. Shifting the position of the beam to a new region of the surface produced the original E_o. The change in E_o was irreversible. The electron beam is likely causing a change in the structure or chemistry of the surface and thus of the work function to which E_o is very sensitive. This type of surface was judged unsuitable for a detector and not studied further.

The values of E_o, Δ, and η are shown for evaporated Au films with and without annealing in Fig. 3 by the solid and dashed lines, respectively. For unannealed films there were many variations from film to film, but the trend was as observed in Fig. 3; generally E_o was higher and the maximum values of Δ and η lower than for annealed films. Very uniform evaporated and annealed films could be obtained for which the parameters did not vary appreciably across the surface. The most sensitive parameter, E_o, varied by ± 0.5 eV as the sample surface was moved a range of 5 mm across the beam.

The three parameters, E_o, Δ, and η, began to change immediately after evaporation in the direction of annealed films. For example, the unannealed results in Fig. 3 are from a film 44 h after evaporation. At $\alpha = 25°$, the values of E_o, Δ, and η from Fig. 3 are 172.3 eV, 1.25 eV, and 0.56×10^{-2}, respectively, compared to 183.3 eV, 0.8 eV, and 0.42×10^{-2} for the same film within a half hour of the time of evaporation. Another film after aging for only 24 h had values of E_o, Δ, and η like an annealed film. Apparently room temperature annealing takes place at a rate which depends on other film parameters such as the thickness. Extensive studies have been made of the optical properties of Au films and have been found to depend on evaporation rate, thickness, and annealing.[15]

The films which had the best detector parameters and which were stable and reproducible were those which we intentionally annealed. The data in Fig. 3 were obtained for a film annealed to 400 °C. Similar results were obtained for a film annealed to 150 °C, although another film did not give the same results until it had been annealed to 225°. Higher temperature annealing of the latter film produced no further change. The possible role of surface contamination in producing these changes was investigated. Closing the valve to the pump to obtain a 2 Langmuir (1L = 10^{-6} Ts) exposure to the background gas produced no change in the film detector parameters. On the other hand, a five-min 150 °C anneal in which the pressure remained less than 6×10^{-11} Torr produced a 50% change in Δ compared to the fresh film. We believe we can rule out residual gas contamination as the cause of change in the detector parameters. There is also the possibility of diffusion of contaminants to the surface of the film. Since any diffusing contaminant would have a lower Z than Au, it would not be likely to cause the factor of two increase in Δ compared with a freshly evaporated film. Low-Z absorbates have been observed to cause large effects in the spin dependent scattering from a W(100) surface.[16] The large changes took place, however, at sharp diffraction features and would not be expected for the diffuse scattering from a polycrystalline film.

The main effect of the annealing is likely to change the polycrystalline structure of the film. Changes in the optical properties, for example, have been correlated with structure changes in the films.[15] A visual observation of the LEED screen indicated only diffuse scattering after as well as before annealing. Corresponding small changes in work function can account for the change in E_o. The slope of the $i^{\uparrow}$ and $i^{\downarrow}$ curves in Fig. 1, absorbed current per incident current per eV, was the same for annealed and unannealed films. The changes observed in Δ and η on annealing a film are due to an increased spin dependence of the scattering from the annealed film. A larger $\eta = |i^{\uparrow} - i^{\downarrow}|/I_o$ automatically gives a larger Δ; this correspondence can be seen in Fig. 3.

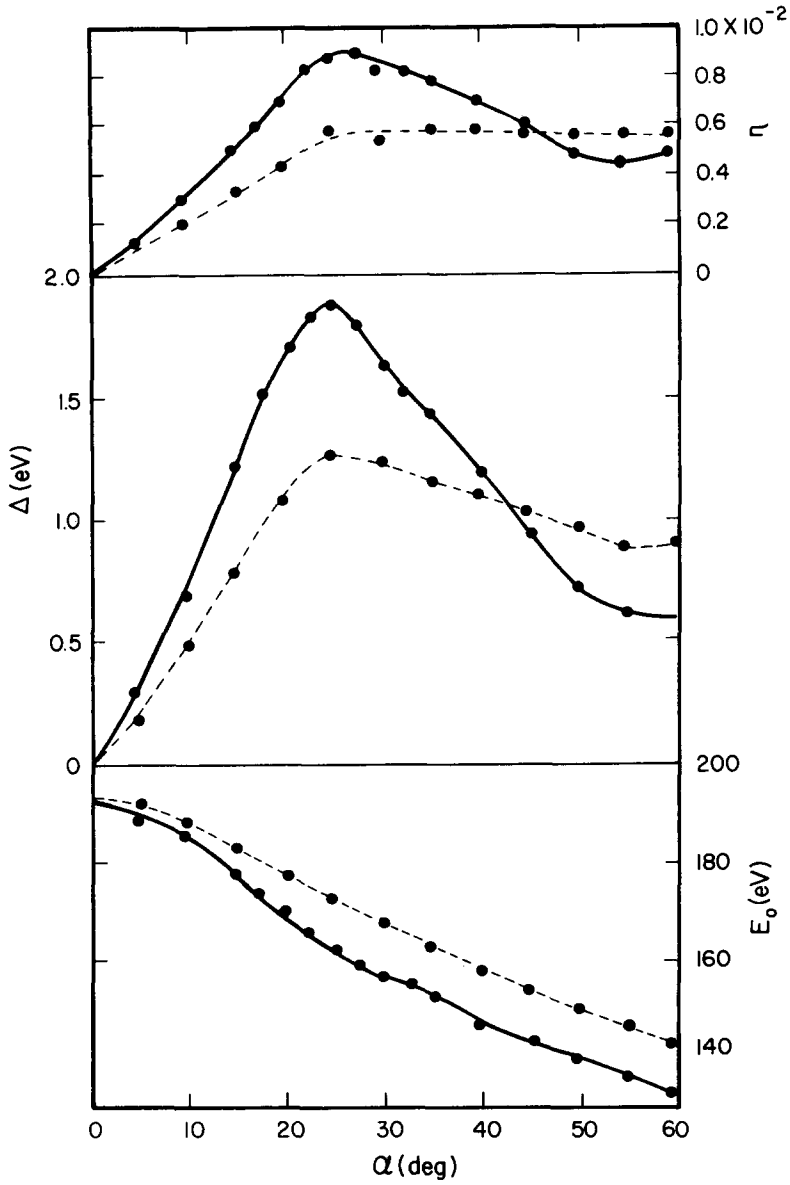

FIG. 3. Measurements of $\eta = |i^{\uparrow} - i^{p}|/I_o$, Δ, and E_o for an annealed evaporated film (solid line) and for an unannealed film (dashed line) are shown as a function of angle of incidence α.

We conclude this section by noting that an annealed Au film, with its high Δ and η at angles of incidence near 25°, is very attractive for an absorbed current spin detector. The annealed films were also quite stable. On a typical film, the values of E_o and Δ were observed to change by ~1 eV and 0.1 eV, respectively, after 12 days. Such variation is sufficiently small for the surface to be useful for a spin detector with only occasional recalibration.

IV. DESIGN CONSIDERATIONS AND APPLICATIONS

From the results of Fig. 3, we expect the operation of the absorbed current spin detector to be sensitive to the angle of incidence, energy, and energy spread of the incident beam. Each of these factors must be handled the same way at the time of calibration and at the time of measurements. In addition to the figure of merit discussed in Sec. II, an important characteristic of a detector that governs its applications is its electron-optical acceptance. This is determined by the conserved phase space product $EA\Omega$, where E is the energy of the beam at the detector, A its cross-sectional area, and Ω its solid angle.

The constraint on the energy spread of the electron beam is not as severe as it might first appear. To the extent that the curves in Fig. 2 are linear, the collected charge from an electron beam with energy spread ΔE about an energy, E, is the same as for a monochromatic beam at the energy, E. Generally, it is desirable to have ΔE the same during calibration and measurement. In the case of a scattered beam, an energy analyzer will be necessary to select the elastically scattered electrons or a particular band of inelastically scattered electrons. The same holds true for an emitted beam, such as for photoemission or field emission.

As discussed above, some of the methods of polarization measurement do not depend sensitively on E_o. Nevertheless, it is desirable to minimize variations in E_o. The energy E_o depends sensitively on the condition

of the detector surface and also varies rapidly with angle. Even in good vacuum, some change in E_o is unavoidable. Very small changes in work function may produce fields that appear sizeable to the large number of low energy secondary electrons which are the dominant factor in determining E_o. For the same reason, the detector surface must be shielded from insulating surfaces which could become charged by the primary beam. For example, an insulating surface can charge to 100 V in a 100-eV beam. If the surface is several centimeters away, the field at the detector may be only a few V/cm and have little effect on electrons at the primary beam energy, but have an enormous effect on the low energy secondaries which determine E_o. With some care in shielding, such charging problems can be eliminated.

Because E_o changes 1 to 1.5 eV per degree change in angle of incidence near $\alpha = 25°$, any measurement averages over some range of E_o as determined by the angular divergence of the beam. This need not adversely affect the measurement as long as the calibration and measurement were made under the same conditions. The same conditions of angular divergence can be maintained by angular collimation in the electron optics preceeding the detector surface.

The factors in the phase space product, $EA\Omega$, are about the same for the absorbed current detector and the PLEED detector.[12,13] A major difference is that the PLEED detector can count single electrons while the absorbed current detector must accumulate charge. The factors in the phase space product of a Mott detector are similar except for the energy which is of order 10^3 greater in the case of a Mott detector. Hence, where the maximum phase space product is required, the Mott detector is advantageous.

The absorbed current spin detector is best suited for measuring low energy electrons where angular resolution of about one degree is needed. The intensity of the incident electron beam must be large enough so that the absorbed current is in the measurement range ($\gtrsim 10^{-17}$ A) of sensitive electrometers. This detector is especially suitable for measuring the change in polarization when a polarized incident beam is scattered. The detector can be moved into the primary beam for calibration and into the scattered beam for measurement. One example of such an application is diffraction from a single crystal surface.

Each measurement puts different demands on a spin detector. The absorbed current spin detector is advantageous for many measurements. It is particularly attractive because it is simple, efficient, and can be made compact and moveable. We expect this new type of electron spin polarization detector will find wide application.

We wish to acknowledge stimulating discussions with H. C. Siegmann and C. J. Powell, and partial support of this work by the Office of Naval Research.

[a] NBS–NRC Postdoctoral Research Associate, 1980–81.

[1] H. C. Siegmann, D. T. Pierce, and R. J. Celotta, Phys. Rev. Lett. **46,** 452 (1981).
[2] M. Erbudak and N. Muller, Appl. Phys. Lett. **38,** 575 (1981).
[3] R. J. Celotta, D. T. Pierce, H. C. Siegmann, and J. Unguris, Appl. Phys. Lett. **38,** 577 (1981).
[4] D. T. Pierce, R. J. Celotta, "Spin Polarization in Electron Scattering From Surfaces," in Adv. Electron. Electron Phys. **56,** 219 (1981).
[5] J. Kessler, *Polarized Electrons* (Springer–Verlag, Berlin, 1976).
[6] L. J. Hayner, Physics **6,** 323 (1935).
[7] B. Kurrelmeyer and L. J. Hayner, Phys. Rev. **52,** 952 (1937).
[8] M. Ziegler, Physics **1,** 1 (1936); **3,** 307 (1936).
[9] W. Schockley and J. R. Pierce, Proc. IRE **26,** 321 (1938).
[10] M. R. Campbell, Proc. Cambridge Philos. Soc. **15,** 310 (1909).
[11] K. A. Brownlee, *Statistical Theory and Methodology in Science and Engineering*, (Wiley, New York, 1960).
[12] J. Kirschner and R. Feder, Phys. Rev. Lett. **42,** 1008 (1979).
[13] G.-C. Wang, R. J. Celotta, and D. T. Pierce, Phys. Rev. B **23,** 1761 (1981).
[14] D. T. Pierce, R. J. Celotta, G.-C. Wang, W. N. Unertl, A. Galejs, C. E. Kuyatt, and S. R. Mielczarek, Rev. Sci. Instrum. **51,** 478 (1980).
[15] J. E. Davey and T. Pankey, J. Appl. Phys. **36,** 2571 (1981), and references therein.
[16] T. W. Riddle, A. H. Mahan, F. B. Dunning, and G. K. Walters, Surf. Sci. **82,** 511 (1979); **82,** 517 (1979).